Body Surface Potential Mapping and Computer Simulation of Human Ventricular Fibrillation

JR Fitz-Clarke, JL Sapp, JW Warren, JC Clements, BM Horáček

Dalhousie University, Halifax, NS, Canada

Abstract

Our aim was to study the electrical characteristics of human ventricular fibrillation (VF) by means of body surface potential mapping and heart-model simulations. We acquired 120-lead ECG data on the chest surface of patients undergoing controlled testing of implantable defibrillators. VF was induced by burst pacing, and ECGs were recorded for 5 to 7 seconds before the device delivered a rescue shock. We then used orthogonal decomposition to characterize spatial and temporal features of ECGs, and inverse solution to derive epicardial potential maps. To gain insight into mechanisms of VF, we used an anisotropic bidomain model of the human ventricular myocardium, featuring 5 ionic currents. The model showed meandering VF scroll waves exhibiting break-up and coalescence according to choice of ionic-current parameters. This combination of experiments and simulations offers a unique perspective on the origin of spatial patterns of ECG during VF.

1. Introduction

Ventricular fibrillation (VF) is sustained in the heart by propagating reentrant circuits of various frequencies that produce irregular body surface electrocardiograms (ECGs). The dynamics of these complex signals are a direct reflection of the underlying electrical status of the myocardium, and might contain useful information for identifying VF subtypes and tailoring management decisions during cardiac resuscitation.

Metrics for characterizing VF signals in the past have included dominant frequencies, fractal dimensions, and scaling exponents obtained almost exclusively in single leads. There have been only a few attempts to study the relationship between ECG signals within multiple leads during VF [1]. Detailed spatial analysis of body-surface ECGs during VF has not been conducted in humans because cardiac arrest is unpredictable, and it is not practical to attach the large lead sets to a patient in advance. Although systems for body surface potential mapping (BSPM) have been used for decades, no such recordings of VF in humans have been reported. Induction of VF for the purpose of testing of implantable cardioverter-defibrillator (ICD) devices in patients is now routine, and offers an opportunity to safely record segments of human VF at high resolution in a controlled environment.

We report on the first detailed body surface potential maps of VF to be recorded and analyzed in humans. We also obtained further insight into the spatiotemporal electrical characteristics of VF and its ECG manifestations on the torso by simulations performed with our large-scale computational model of the human heart.

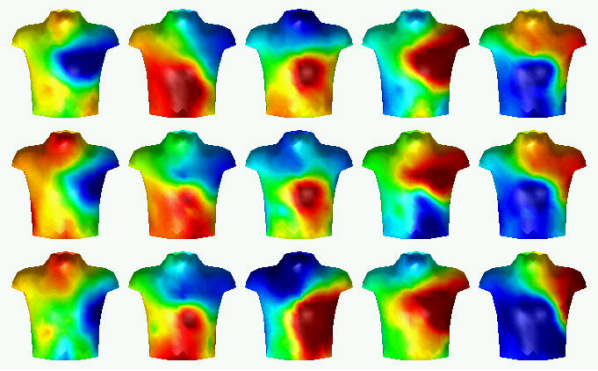

Figure 1. Body surface potentials during VF on the anterior torso of patient #2. Sequence is shown in rows, at 40-ms intervals; positive potentials, yellow to red; negative potentials, green to blue.

2. Methods

2.1. VF recordings

Patients referred for ICD implantation were recruited into this study after providing informed consent. Electrode strips (FoxMed, Idstein, Germany) were placed over the anterior and posterior chest in standard positions used at our institution [2], with the exception that electrodes were not placed within the left subclavian surgical field, nor at the usual sites of the adhesive defibrillation pads used for delivering back-up rescue shocks. After implantation of the ICD under general anesthesia, VF was induced by burst pacing via a catheter

placed in the right ventricular apex. A 120-lead ECG mapping system (BioSemi, Amsterdam) was used to record ECGs at 2000 samples/sec/channel for 5 to 7 seconds while the ICD charged before delivering an internal rescue shock.

BSPM recordings from 6 patients were obtained in this manner, and 3 have been analyzed so far. ECGs were processed off-line to correct for pacing-induced transient baseline deviation, and to interpolate spatial potential distributions in areas not covered by electrodes, yielding ECG signals for 352 torso-surface nodes [2].

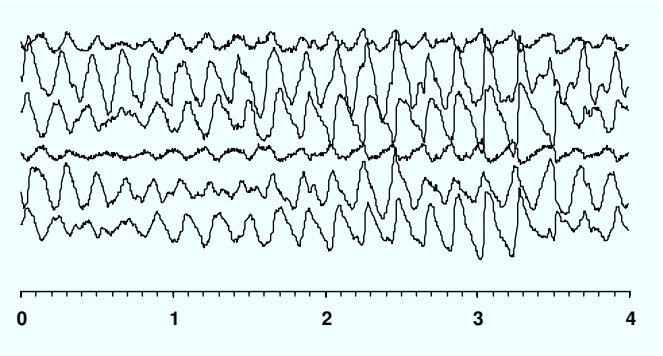

Figure 2. ECG signals in selected leads for induced VF. These tracings are continuous recordings for 6 scalar leads of VF depicted in Fig. 1 as instantaneous body-surface potential maps; time-scale is in seconds.

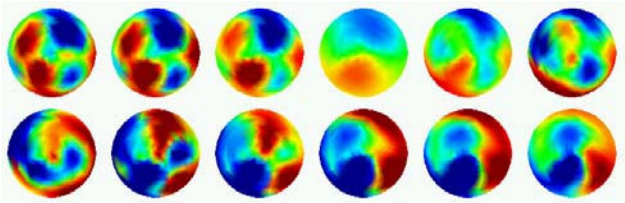

Figure 3. Apical view of epicardial potential maps of VF at 10-ms intervals. These maps, arranged in rows, were obtained by inverse solution from instantaneous BSPM distributions of VF shown in Fig. 1; apex is at the centre, the anterior wall on top, the inferior wall on bottom, the right ventricular free wall to the left, the left ventricular free wall to the right, and the AV ring along the rim.

2.2. Inverse solution

Maps of epicardial potentials were calculated at each time instant of recorded body-surface ECG signals by applying the electrocardiographic inverse solution; this approach is also referred to as electrocardiographic imaging [3]. For all 3 analyzed patients, we used the same homogeneous model of the torso, with 352 body-surface nodes and 202 epicardial-surface nodes to perform the inverse solution by means of boundary-element method [4]. Second-order Tikhonov regularization was used, with an optimal regularization parameter chosen by the L-curve method [5]. The resulting epicardial-surface potential distributions were mapped onto the projection of the epicardial surface (Fig. 3).

2.3. Principal component analysis

Principal component analysis of BSPMs in space and time was performed using the Karhunen-Loéve transform (KLT) to extract the optimal orthogonal eigenvector set. Using this technique, the BSPMs can be represented as a linear sum of N orthonormal basis vectors φ_i

$$P_N = \sum_{i=1}^{N} \alpha_i \varphi_i , \qquad (1)$$

with time-dependent coefficients α_i. The KLT allows determination of the spatial pattern basis set φ_i that minimizes the error in matching P_N with the original data set P. This can be shown to be equivalent to the eigenvalue problem

$$\mathbf{K}\, \varphi_j = \lambda_j \varphi_j , \qquad (2)$$

where **K** is the covariance matrix of the data P, and λ_j are the corresponding eigenvalues [6,7].

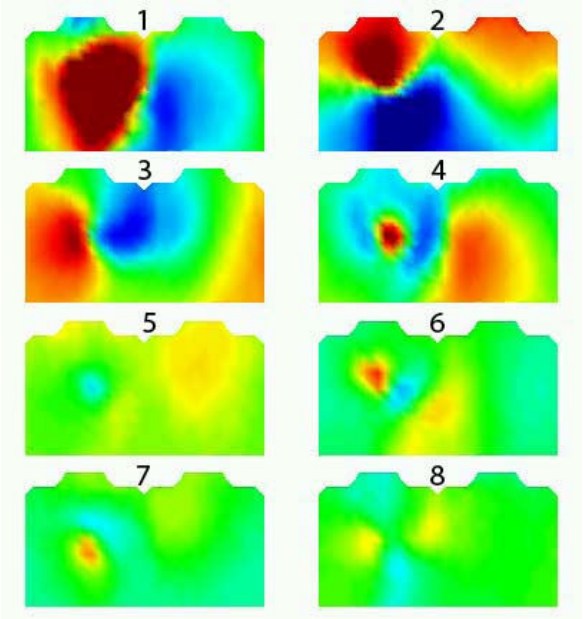

Figure 4a. The first 8 eigenvectors of the orthonormal set, representing spatial patterns of VF shown in Fig. 1 on the anterior (left side of each frame) and posterior (right side) surface of the torso.

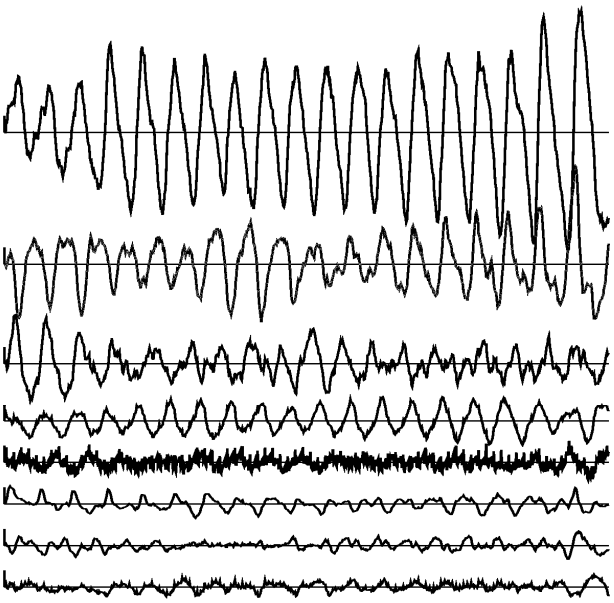

Figure 4b. The first 8 eigenfunctions (time-dependent coefficients α_i) of the orthonormal set, representing temporal patterns of VF shown in Fig. 1 for 4 seconds of recorded ECG data.

2.4. Heart-model simulations

We used an anatomically and physiologically realistic computational model of the human ventricular myocardium as an adjunct to aid in analysis and interpretation of VF dynamics. The model's structure is derived from post mortem sections of the human heart and incorporates accurately-represented transmural fibre rotation [8]. The ionic model of the cardiac action potential is qualitatively based on the phase 1 Luo-Rudy formulation [9]. The essential set of ionic currents (I_{Na}, I_{Ca}, I_K, I_{KT}, and I_{to}) were retained to capture realistic restitution properties of endocardial, epicardial, and M cells tailored to human ventricular myocardium. This modified model allows the option of simulating various pharmacological interventions mimicking action of antiarrhythmic drugs [10]. All numerical simulations of VF were displayed using animation to track propagating wave fronts and scroll wave vortex filaments meandering throughout the ventricles; this was made possible by MATLAB (The MathWorks, Natick, MA) visualization software.

3. Results

BSPM data revealed regions of positive and negative potentials that moved rapidly over the torso in organized patterns reflecting contributions of the multiple dominant dipoles to the ECGs (Fig. 1). Signals in individual leads appeared fairly regular after initial VF induction (Fig. 2), exhibiting a peak frequency at about 5 Hz, consistent with other studies investigating early human VF [11]. All VF recordings showed considerable spatial coherence between leads, and the presence of intermittent dominant rotational components appearing to revolve around the torso in various planes.

Examples of epicardial maps calculated by inverse solution are shown in Fig. 3. These maps provide a necessary link between body-surface ECG measurements and heart-model simulations. Spatial and temporal patterns of VF (patient #2) obtained by KLT are shown in Figs. 4a & 4b as sets of eigenvectors and eigenfunctions, respectively. In this case, the first four eigenvectors accounted for, respectively, 55.7%, 25.7%, 9.8%, and 4.8% of pattern variance over the 4-second interval.

Heart-model simulations produced highly dynamic patterns similar to those observed in isolated perfused dog hearts [12]. Spiral wave segments could be followed between time frames, but it was often difficult to track the survival of any given reentrant circuit beyond a few rotations, due to dynamic complexity, core meander, and twisting, consistent with reports based on epicardial maps [13]. Since the wave fronts are scroll waves rotating around filaments in three dimensions, epicardial breakthrough can appear to be focal, as was seen in frames where wave-front rings appeared on the surface, originating from wave propagation inside the wall, and subsequently radiated outward. Epicardial focal patterns such as these are sometimes seen during VF, giving the appearance of ectopic activation. Propagating waves exhibited break-up and coalescence according to choice of ionic-current parameters. An example of model-simulated epicardial activity is shown for nominal ionic current parameters in Fig. 5. This simulated VF activity had a mean cycle length of about 180 ms, consistent with the dominant frequency of 5 Hz seen in the human ECGs shown in Fig. 2 obtained from the BSPM study.

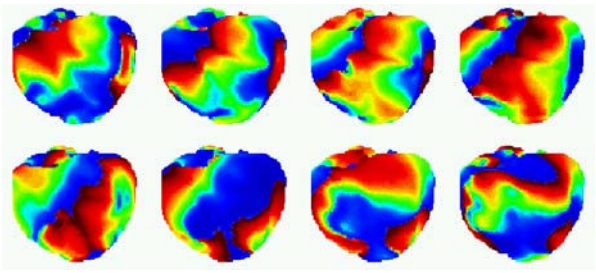

Figure 5. Computer simulation of VF showing trans-membrane potentials on the anterior epicardial surface in 10-ms frames. Action potential wave fronts are shown in dark red, and fully recovered tissue is shown in blue.

4. Discussion and conclusions

To our knowledge, our BSPM recordings of VF are the first to be obtained in human subjects. For ethical reasons, VF was not permitted to extend beyond the usual time for ICD charging and shock delivery, which was typically about 7 to 10 seconds. Useable VF data segments after removal of transient pacing artifacts were therefore limited to about 5 seconds after VF induction. During this period, before the development of significant ischemia, electrical activity was still relatively organized. VF signals exhibited a high degree of coherence between leads, producing spatial patterns that resembled those produced by multiple rotating dipoles of varying strengths and orientations.

Calculated epicardial maps obtained by inverse solution did not resolve clearly discernible underlying focal or reentrant wave activity. This was to be expected, since fibrillation is known to have complex three-dimensional structure within the thickness of the ventricular walls that cannot be adequately captured in a two-dimensional projection onto the epicardial surface.

There were some limitations to this study. Constraints related to patient safety prevented electrodes from being placed on all desired regions of the torso. In particular, the area directly over the heart could not be mapped at high resolution, due to the presence of the anterior defibrillation pad. Spatial reconstruction of body surface potential distributions from individual leads was found to be sensitive to uncorrelated baseline drift and signal noise that could not be filtered out entirely. It is also conceivable that pacing-induced VF recorded in this study might not be dynamically equivalent to VF occurring spontaneously with cardiac arrest.

Our computer model of ventricular myocardium, featuring a simplified ionic model of ventricular action potential, proved capable of simulating a variety of VF subtypes through manipulation of ionic conductances and time constants. Simulated epicardial maps, ECG frequency spectra of VF, and the effects of drugs were consistent with those previously obtained experimentally. State-of-the-art visualization software allowed an unprecedented insight into genesis of VF patterns from scroll waves rotating around filaments within the ventricular wall to epicardial potential distributions and body-surface electrocardiographic distributions.

Acknowledgements

Support for this study was provided by grants from the Canadian Institutes of Health Research, the Nova Scotia Health Research Foundation, the Heart and Stroke Foundation of Nova Scotia, and from Medtronic.

References

[1] Clayton RH, Murray A, Campbell RWF. Analysis of the body surface ECG measured in independent leads during ventricular fibrillation in humans. Pacing Clin Electrophysiol 1995;18:1876-81.

[2] Horáček BM, Warren JW, Penney CJ, MacLeod RS, Title LM, Gardner MJ, Feldman CL. Optimal electrocardiographic leads for detecting acute myocardial ischemia. J Electrocardiol 2001;34(Suppl):97-111.

[3] Ramanathan C, Ghanem RN, Jia P, Ryu K, Rudy Y. Noninvasive electrocardiographic imaging for cardiac electrophysiology and arrhythmia. Nature Med 2004;10:422-8.

[4] Horáček BM, Clements JC. The inverse problem of electrocardiography: A solution in terms of single- and double-layer sources on the epicardial surface. Math Biosci 1997;144:119-54.

[5] Hansen PC, O'Leary DP. The use of the *L*-curve in the regularization of discrete ill-posed problems. SIAM J Sci Statist Comput 1993;14:1487-503.

[6] Lux RL, Evans AK, Burgess MJ, Wyatt RF, Abildskov JA. Redundancy reduction for improved display and analysis of body surface potential maps. I. Spatial compression. Circ Res 1981;49:186-96.

[7] Hubley-Kozey CL, Mitchell LB, Gardner MJ, Warren JW, Penney CJ, Smith ER, Horáček BM. Spatial features in body-surface potential maps can identify patients with a history of sustained ventricular tachycardia. Circulation 1995;92:1825-38.

[8] Hren R. A Realistic Model of Human Ventricular Myocardium: Application to the Study of Ectopic Activation. PhD Thesis. Dalhousie University, 1996.

[9] Luo C-H, Rudy Y. A model of the ventricular cardiac action potential: depolarization, repolarization, and their interaction. Circ Res 1991;68:1501–26.

[10] Fitz-Clarke JR. Spatiotemporal Dynamics of Ventricular Fibrillation in a Three-Dimensional Anisotropic Heart Model. PhD Thesis. Dalhousie University, 2003.

[11] Nash MP, Mourad A, Clayton RH, Sutton PM, Bradley CP, Hayward M, Paterson DJ, Taggart P. Evidence for multiple mechanisms in human ventricular fibrillation. Circulation 2006; 114:536-42.

[12] Witkowski FX, Leon LJ, Penkoske PA, Giles WR, Spano ML, Ditto WL, Winfree AT. Spatiotemporal evolution of ventricular fibrillation. Nature 1998;392:78-82.

[13] Gray RA, Pertsov AM, Jalife J. Spatial and temporal organization during cardiac fibrillation. Nature 1998; 392:75-8.

Address for correspondence

John R. Fitz-Clarke, MD, PhD
Department of Physiology and Biophysics
Sir Charles Tupper Medical Building
Dalhousie University
Halifax, Nova Scotia, Canada B3H 4H7
jfitzclarke@eastlink.ca